EPJ Web of Conferences **346**, 01003 (2026) https://doi.org/10.1051/epjconf/202634601003
RFPPC2025

Beam Tracing in Phase Space: Paraxial Description of High-Frequency Wave Beams in Turbulent Plasmas

Omar Maj[1,*], *Hannes* Weber[1], and *Emanuele* Poli[1]

[1]Max Planck Institute for Plasma Physics, Boltzmannstrasse 2, 85747, Garching, Germany.

Abstract. The averaged wave energy density carried by an electron-cyclotron wave beam in a turbulent plasma can be computed by solving numerically the wave kinetic equation. This approach however can be computationally demanding due to the high dimensionality of the problem. In this work, we show how ideas from paraxial optics can be applied to construct an approximate solution of the wave kinetic equation. This construction requires only the solution of a small system of ordinary differential equations.

1 Introduction

Asymptotic methods based on the short wavelength limit constitute the main computational tools for the description of high-frequency wave beams in fusion plasmas. One such method, namely the paraxial Wentzel-Kramers-Brillouin (pWKB) or beam-tracing method [1–3], has been proven to be computationally efficient and physically insightful for both electron cyclotron [4, 5] and lower hybrid waves [1, 6], as well as for plasma diagnostics [7]. The pWKB method, however, cannot be directly applied to plasmas with density fluctuations, yet the effects of such density fluctuations can be a concern for the beam quality in large tokamaks such as ITER and need to be accounted for [8]. Understanding the effects of fluctuations has generated a considerable volume of both experimental and theoretical work in the last years. A thorough review of the available results is beyond the scope of this paper. As an entry point, we refer the reader to the the work of Tsironis et al. [9] and Sysoeva et al. [10] for theory and simulations, and to Chellaï et al. [11] and Brookman et al. [12] for experimental studies.

In this context, we have proposed an approach based on the direct numerical solution of a version of McDonald's wave kinetic equation [13], which describes the Wigner function of the wave electric field averaged over the statistical ensemble of density fluctuations. This numerical approach has been implemented in the `WKBeam` code [14, 15] and it has already been used in a number of studies [16, 17]. It is however computationally much more expensive than the standard pWKB method.

In this paper, we show that some of the ideas at the basis of the pWKB method can be transferred to the wave kinetic equation in order to obtain a simpler and physically more insightful description of the wave beam, as compared to the method adopted in `WKBeam`. The simplification stems from the fact that the solution of the wave kinetic equation in the geometric-optics phase space is concentrated around a reference trajectory [18, 19] opening the possibility to develop a phase-space beam-tracing method. More precisely, we construct a paraxial approximation of the solution of the wave kinetic equation. However, we shall restrict the scope of our work to the case of density fluctuations that fall well within the diffusive scattering regime [19, 20]. The diffusive regime is most relevant to large machines such as ITER and DEMO, and it implies some simplifications in the mathematical form of the scattering operator that accounts for the effects of density fluctuations in the wave kinetic equation.

A similar method has been developed for wave packets [21]: the Wigner function is approximated by a Gaussian function in phase space, and equations are derived for the center of the Gaussian and a positive-definite, real symmetric matrix G, which is defined as the inverse of the covariance matrix of the Gaussian. One finds that a Gaussian Wigner function corresponds to a pure wave packet if and only if the matrix G is symplectic. Otherwise, the Gaussian Wigner function describes a "mixed state", i.e., a statistical ensemble of wave packets.

The case of wave beams addressed here is somewhat more complicated since, differently from wave packets, the field is delocalized in one direction, i.e., the propagation direction (cf. section 1.1 below), and thus the wave field is not squared integrable. As a result, the analogous of the matrix G is singular (it has a zero eigenvalue) and therefore cannot be symplectic (since symplectic matrices have necessarily determinant ± 1). Dealing with this singularity is one of the main technical aspects of our work. Nonetheless, we discover a similar relation between pure wave beams and the symplectic structure of the geometrical-optics phase space. We shall see that in random media, density fluctuations destroy this relation. Therefore the Wigner function of the beam in a fluctuating plasma, in general, represents a statistical ensemble of beams, rather than a single beam with a well defined phase

*Corresponding author: omar.maj@ipp.mpg.de

and cross-section. We shall still be able to define the width of the average energy distribution, but of course not the phase. The "purity" of the beam can also be quantified in terms of an entropy function [18].

In the remaining part of this introduction, we briefly recall the pWKB method (section 1.1) and the wave kinetic equation (section 1.2). The pWKB method will be used to construct a reference solution for beams in quiescent plasmas, i.e. when electron density fluctuations can be neglected; the wave kinetic equation will be the starting point for the derivation of the proposed method. The aim of this paper is documenting some of the technical aspects of this derivation, particularly for the case of beams in a quiescent plasma (section 2), which allows us to establish the basis of the method. For the general case of beams in random media, we shall not give the details, but focus instead on the construction of the paraxial solution and discuss a numerical example (section 3). For quiescent plasmas we shall see that pure beams are preserved and test numerically the relation between pure beams and the symplectic form. For fluctuating plasmas, we compare the paraxial solution to the results of the `WKBeam` code. We find that the paraxial solution of the wave kinetic equation, in the considered cases, coincides with the pWKB solution within the numerical error for the cases without fluctuations, and provides a reasonably good approximation in the diffusive regime. As expected, the approximation becomes poorer as we move away from the diffusive regime.

1.1 Standard beam-tracing equations

The paraxial WKB method relies on searching for appropriate beam-following coordinates [3]. Differently from other ways to implement the paraxial approximation [22], these coordinates are not constructed *ad hoc*, but they are determined from the wave equation in a self-consistent way. This is the approach that we shall follow for the wave kinetic equation in sections 2 and 3, therefore we briefly recall the idea.

For the specific case of a Gaussian beam of given angular frequency $\omega > 0$, the pWKB ansatz for the wave electric field amounts to [3, eq. (16) with $m = n = 0$]

$$E^\kappa(x) = a(x)e^{i\kappa s(x) - \kappa u(x)^2/2} + O(1/\sqrt{\kappa}), \quad \kappa \to +\infty, \quad (1)$$

where $x = (x^i)_{i=1}^d$ are coordinates in a Cartesian reference frame normalized to the scale length $L > 0$ of the medium variations, $d \geq 2$ is the dimension of the physical domain ($d = 3$ for the physical three-dimensional domain), a is the complex vector-valued amplitude (including the polarization vector), s is the phase (eikonal) function, and $u = (u^\alpha)_{\alpha=1}^{d-1}$ are the (*a priori* unknown) coordinates spanning the cross-section of the beam. The parameter $\kappa = \omega L/c$, with c the speed of light in vacuum, is the large parameter that controls the high-frequency limit $\kappa \to +\infty$, also known as *semiclassical limit*. One can interpret $\phi(x) = u(x)^2/2$ as an imaginary part of a complex phase, which grows quadratically in u. The key point of the paraxial method consists in the observation that where $u \neq 0$, the wave field is exponentially small in the limit $\kappa \to +\infty$, i.e., the field is concentrated on a curve $\mathcal{R} = \{x : u(x) = 0\}$, which is however *a priori* unknown (since the coordinates are unknown). If τ is another curvilinear coordinate such that $(\tau, u^1, \ldots, u^{d-1})$ is a coordinate system near $\mathcal{R}$, we have the parameterization $\mathcal{R} = \{x = x_0(\tau)\}$.

The paraxial approximation relies on the inequality [3] (cf. also Maslov [23, Ch. 1, section 3]),

$$\left|(u^1)^{n_1} \cdots (u^{d-1})^{n_{d-1}} e^{-\kappa u^2/2}\right| \leq C\kappa^{-n/2}, \quad n = \sum_\alpha n_\alpha, \quad (2)$$

with constant C depending only on the integer exponents $n_1, \ldots, n_{d-1} \geq 0$. This is another way to say that the field is concentrated on $\mathcal{R}$ and justifies the Taylor expansions

$$\begin{aligned} a(x) &= a_0(\tau) + O(|x - x_0|), \\ s(x) &= s_0(\tau) + N^0(\tau) \cdot (x - x_0(\tau)) \\ &\quad + \tfrac{1}{2}(x - x_0(\tau)) \cdot S(\tau)(x - x_0(\tau)) + O(|x - x_0|^3), \end{aligned}$$

where $a_0(\tau) = a(x_0(\tau))$ and $s_0(\tau) = s(x_0(\tau))$ are the amplitude and the eikonal evaluated on the curve $\mathcal{R}$, respectively, $N^0(\tau) = \nabla s(x_0(\tau))$ is the local refractive index vector (i.e., the local wave vector normalized to ω/c), and $S(\tau) = D^2 s(x_0(\tau))$ is the Hessian matrix of the eikonal. We also have $u^\alpha(x) = (x - x_0(\tau)) \cdot \nabla u^\alpha(x_0(\tau)) + O(|x - x_0|^2)$, and

$$u(x)^2 = (x - x_0(\tau)) \cdot \Phi(\tau)(x - x_0(\tau)) + O(|x - x_0|^3),$$

where the symmetric positive semi-definite matrix $\Phi(\tau)$ has components $\Phi_{ij}(\tau) = \partial_{x^i} u^\alpha(x_0(\tau))\delta_{\alpha\beta}\partial_{x^j} u^\beta(x_0(\tau))$. (Einstein summation convention is used throughout this paper.) Estimate (2) essentially implies that the remainders in the foregoing expansions amount to corrections of order $1/\sqrt{\kappa}$ in the electric field. It is now sufficient to know $z_0 = (x_0, N^0)$, $\Psi = S + i\Phi$, s_0, and $a_0 = e(z_0)A_0 e^{i\vartheta_0}$, where $e(z)$ is the polarization unit vector of the considered wave mode at the phase-space point $z = (x, N)$, A_0 is the scalar real-valued amplitude of the wave field, and ϑ_0 is the sum of geometric phases due to the transport of the polarization vector and the Gouy phase shift. The explicit form of ϑ_0 will not be needed in this work, for reasons that will become clear below; therefore, we do not give the details on the calculation of ϑ_0. For the remaining quantities, the pWKB method yields the following systems of ordinary differential equations (ODEs), referred to as beam-tracing equations,

$$\frac{dz_0}{d\tau} = -J_c \nabla_z H(z_0), \quad H(z_0) = 0, \quad (3a)$$

$$-\frac{d\Psi}{d\tau} = H_{xx} + \Psi H_{Nx} + H_{xN}\Psi + \Psi H_{NN}\Psi, \quad (3b)$$

$$0 = \Psi \nabla_N H(z_0) + \nabla_x H(z_0), \quad (3c)$$

$$\frac{ds_0}{d\tau} = N^0 \cdot \nabla_N H(z_0), \quad (3d)$$

$$\frac{dA_0}{d\tau} = -(\tfrac{1}{2}\operatorname{div} V + \gamma(z_0))A_0, \quad (3e)$$

where

$$J_c = \begin{pmatrix} 0 & -I \\ I & 0 \end{pmatrix}$$

is the canonical Poisson tensor (the inverse of the canonical symplectic form), and $H(z) = H(x, N)$ is the geometrical optics Hamiltonian as a function of position x and refractive index N. The subscripted variables denote differentiation, e.g., $(H_{xN})_i^j = \partial^2 H/\partial x^i \partial N_j$, all derivatives of H are assumed to be evaluated at $z = z_0$, $\operatorname{div} V = \operatorname{tr}(H_{xN} + H_{NN} S)$ is the divergence of the (normalized) group velocity, and γ is the absorption coefficient.

In particular, the curve $z_0 = (x_0, N^0)$ in the position-refractive-index phase space satisfies the standard geometrical optics equations (3a). These are Hamilton's equations with the additional condition that the Hamiltonian must attain the value $H = 0$, which is the dispersion relation of the considered wave mode. As a consequence the curve $\mathcal{R}$ is called the *reference ray*, since it is indeed a particular geometrical optics ray. The interaction between $S = \operatorname{Re}\Psi$ and $\Phi = \operatorname{Im}\Psi$ via the nonlinear term in the matrix Riccati equation (3b) accounts for diffraction effects [24]. The Riccati equation is coupled to the algebraic constraint (3c), which however is compatible, i.e. it is automatically satisfied if the initial condition $\Psi(0)$ satisfies it. At last, the equations for the eikonal s_0 and the scalar amplitude A_0 are identical to the corresponding equations in geometrical optics, but here the divergence of the group velocity depends on the matrix S, which is not the same as in geometrical optics, as it is affected by diffraction. We recall that physically the matrices $S(\tau)$ and $\Phi(\tau)$ encode information on the curvature of the phase fronts and the beam width at the point $z = z_0(\tau)$, respectively.

We note that equation (3c) implies $\Phi\nabla_N H(z_0) = 0$, and thus Φ is necessarily a singular matrix. This expresses the fact that the Gaussian envelope $e^{-\kappa u^2/2}$ in equation (1) localizes the wave field only in the two dimensions transversal to the reference ray.

1.2 The wave kinetic equation for beams in turbulent plasmas

In a statistical description of fluctuations, we assume that the electron density is the sum of a smooth equilibrium $n_{e,0}$ plus a random time-independent perturbation $\tilde{n}_e = n_{e,0}\mu/\sqrt{\kappa}$, where μ is a random field, representing the density fluctuations relative to the equilibrium. The scaling with $\sqrt{\kappa}$ is a standard assumption [25]. The physical fluctuations are of course time dependent, but the idea is that, under suitable conditions, the time-average of a quantity of interest, computed with the physical density, is equal to the expectation value of the same quantity computed with the random density field.

As for the statistics of the random perturbation, we assume that μ has zero average, $\mathbb{E}(\mu(x)) = 0$. In addition, we only need to provide the two-point correlation function $C_\mu(x, x') = \mathbb{E}((\mu(x)\mu(x'))$, for which we choose

$$C_\mu(x + \tfrac{s}{2}, x - \tfrac{s}{2}) = F(x)^2 \exp\big[- s \cdot \Xi(x) s\big]. \quad (4)$$

Here $\mathbb{E}$ denotes the expectation value operator (i.e. the average over a large number of realizations of the random field), $F(x)$ is the root mean square of $\mu(x)$, and $\Xi(x)$ is a generic symmetric positive definite matrix. In practice, for the physical three-dimensional models, we choose $\Xi(x) = (L_\parallel(x)^{-2} - L_\perp(x)^{-2}) e_\parallel(x)\, {}^t e_\parallel(x) + L_\perp(x)^{-2} I$, where $e_\parallel(x)$ is the unit vector in the direction of the magnetic field at x, ${}^t e_\parallel(x)$ is its transpose (throughout this paper a superscripted t on the left of the symbol denotes the transpose), and $L_\parallel(x)$, $L_\perp(x)$ are the correlation lengths of the fluctuations in the directions parallel and perpendicular to the local magnetic field, respectively.

Since μ is time-independent, we can still solve the wave equation in the frequency domain, as in the case of a quiescent plasma. The solution E^κ is now a random field since the coefficients of the wave equation depend on the random perturbation μ. Specifically, for any realization of the random field μ we have a corresponding solution E^κ, and we want to compute an approximation of the correlation matrix $\rho^\kappa(x, x') = \mathbb{E}(E^\kappa(x) E^\kappa(x')^*)$. It turns out that it is more convenient to consider the associated Wigner matrix $W^\kappa(x, N)$ defined so that

$$\rho^\kappa(x, x') = \Big(\frac{\kappa}{2\pi}\Big)^d \int e^{i\kappa(x-x')\cdot N} W^\kappa(\tfrac{x+x'}{2}, N) dN, \quad (5)$$

In the semiclassical limit $\kappa \to +\infty$, we find

$$W^\kappa = \sum_j w_j^\kappa e_j\, {}^t e_j + O(1/\kappa),$$

where the index j runs over the wave modes (O-mode and X-mode), $e_j(x, N)$ is the mode polarization unit vector (defined as in geometrical optics), and w_j^κ is the scalar Wigner function associated to the mode. Upon neglecting the coupling of the modes due to the fluctuations, each Wigner function w_j^κ is independent of the others and solves a constrained transport equation [15], i.e. (dropping the index j for brevity)

$$\begin{cases} \{H, w^\kappa\} = -2\gamma w^\kappa + S^\kappa(w^\kappa), \\ \quad H w^\kappa = 0, \end{cases} \quad (6)$$

where $\{f, g\} = \nabla_z f \cdot J_c \nabla_z g$ is the canonical Poisson bracket on the geometrical-optics phase space, H and γ are the same Hamiltonian and absorption coefficient discussed in section 1.1, and the effect of fluctuations is accounted for by the scattering operator

$$S^\kappa(w^\kappa) = \int [\sigma^\kappa(x, N', N) w^\kappa(x, N') \\ - \sigma^\kappa(x, N, N') w^\kappa(x, N)] dN', \quad (7)$$

with scattering cross-section

$$\sigma^\kappa(x, N, N') = (\tfrac{\kappa}{2\pi})^d \Gamma^\kappa(x, N - N') \\ \times \left| e(x, N)^* (\varepsilon_{\mathrm{cold}}(x) - I) e(x, N') \right|^2 2\pi\delta(H(x, N'))$$

depending on the two-point correlation function (4) via its Wigner transform

$$\Gamma^\kappa(x, N) = \int e^{-i\kappa N\cdot s} C_\mu(x + \tfrac{s}{2}, x - \tfrac{s}{2}) ds.$$

Here δ denotes the Dirac's distribution, and $\varepsilon_{\mathrm{cold}}(x)$ is the cold-plasma dielectric tensor, that is, we assume that hot-plasma effects are negligible in the regions where the density fluctuations are important. On the other hand, the

Hamiltonian H and the absorption coefficient γ can in principle include hot-plasma effects, even though for simplicity H in `WKBeam` is computed using the cold-plasma approximation.

We note that in equation (6) the constraint $Hw^\kappa = 0$ imposes $w^\kappa = 0$ where $H \neq 0$, i.e. w^κ is localized on the surface in phase space where the dispersion relation of the mode, $H(x, N) = 0$, is satisfied. This means, in particular, that a solution of (6) is necessarily singular, $w^\kappa \propto \delta(H)$. We also note that the definition of μ and Γ^κ used here are based on the relative density fluctuations, differently from Ref. [15]. Moreover in equation (22) of Ref. [15], the factor $(\kappa/2\pi)^d$ was missed.

Equation (6) is the wave kinetic equation solved by the `WKBeam` code [15]. Numerical experiments show that the Wigner function w^κ remains concentrated around a solution of ray equations (3a) in phase space. The aim of this work is the construction of an approximate solution for w^κ obtained by applying a modified version of the paraxial method outlined in section 1.1.

2 Phase-space beam tracing in quiescent plasmas

As a first step we consider the case of a quiescent plasma, that is we neglect the random density fluctuations. Then the wave kinetic equation (6) reduces to

$$\{H, w^\kappa\} = -2\gamma w^\kappa, \qquad Hw^\kappa = 0. \tag{8}$$

This equation describes the transport of the Wigner function w^κ by the Hamiltonian vector field in equations (3a), subject only to damping described by γ. Let (τ, h, ζ) be coordinates such that $\tau(z)$ takes values in the interval $0 \leq \tau \leq \tau_{\max}$, $h(z) = H(z)$ is given by the Hamiltonian with $\{H, \tau\} = 1$, and $\zeta(z) = (\zeta^\mu(z))_{\mu=1}^{2d-2}$ with $\{H, \zeta^\mu\} = 0$ for all μ. If such coordinates exist, then (8) can be written as

$$\partial_\tau w^\kappa = -2\gamma w^\kappa, \qquad hw^\kappa = 0,$$

where we used the same symbol w^κ to denote the Wigner function in the new coordinate system. This form of the equation can be solved analytically, and the solution is

$$w^\kappa(\tau, h, \zeta) = (2\pi/\kappa)\delta(h)w_*^\kappa(\zeta)e^{-2\int_0^\tau \gamma_H(\tau', \zeta)d\tau'}, \tag{9}$$

where $\gamma_H = \gamma|_{\{H=0\}}$, and $w_*^\kappa(\zeta)$ is an arbitrary boundary condition prescribed on the hypersurface defined by the conditions $\tau(z) = 0$ and $h(z) = H(z) = 0$. As expected, w^κ is singular, as it involves a Dirac's distribution.

From the assumptions on this specific system of curvilinear coordinates, we can deduce an equation for the transformation $z(\tau, h, \zeta)$. The covariant basis vector $\partial_\tau z$ must be orthogonal to the contravariant basis vectors ∇H and $\nabla\zeta^\mu$ for all μ; since $\{H, H\} = 0$ and $\{H, \zeta^\mu\} = 0$ for all μ, we also have that $-J_c\nabla H$ is orthogonal to ∇H and $\nabla\zeta^\mu$, hence $\alpha\partial_\tau z = -J_c\nabla H(z)$, with α a scalar function to be determined. In order to find the proportionality function α, we use the condition $\{H, \tau\} = 1$, which amounts to $1 = (-J_c\nabla H)\cdot\nabla\tau = \alpha\partial_\tau z\cdot\nabla\tau = \alpha$, since coordinates must satisfy $\partial_\tau z\cdot\nabla\tau = 1$. We conclude that $\alpha = 1$, and $\partial_\tau z = -J_c\nabla H(z)$, that is, a coordinate system with the desired properties must be such that the τ-lines, $\tau \mapsto z(\tau, h, \zeta)$, solve Hamilton's equations. This gives us a way to construct the coordinates starting from a given surface where $\tau = 0$. However, the full, explicit construction of the coordinates will not be needed in the paraxial approach.

2.1 Paraxial approximation of the Wigner function

As we shall see later, for Gaussian beams, the boundary datum w_*^κ can be taken Gaussian, i.e.,

$$w_*^\kappa(\zeta) = W_0^\kappa e^{-\kappa|\zeta|_g^2},$$

where $g = (g_{\mu\nu})_{\mu,\nu=1}^{2d-2}$ is a symmetric positive-definite matrix, $|\zeta|_g^2 = \zeta\cdot g\zeta = g_{\mu\nu}\zeta^\mu\zeta^\nu$, and W_0^κ is a normalization constant. With this boundary condition, w^κ is concentrated on the curve $\mathcal{O} = \{z = z_0(\tau)\}$ defined by the conditions $H(z) = 0$ and $\zeta(z) = 0$. One may think of the coordinates ζ as the phase-space analogous of the coordinates u in the pWKB method, and of the curve $\mathcal{O}$ as the phase-space analogous of the reference ray $\mathcal{R}$, cf. section 1.1. Near $\mathcal{O}$ we have $\zeta^\mu(z) = (z - z_0)\cdot\nabla\zeta^\mu(z_0) + O(|z - z_0|^2)$, and thus

$$g_{\mu\nu}\zeta^\mu(z)\zeta^\nu(z) = (z - z_0)\cdot G(z - z_0) + O(|z - z_0|^3),$$

where we have introduced the $2d \times 2d$ matrix

$$G(\tau) = g_{\mu\nu}\nabla\zeta^\mu(z_0(\tau)) \otimes \nabla\zeta^\nu(z_0(\tau)).$$

The symbol $\otimes$ denotes the dyadic product. By definition $G(\tau)$ is symmetric, positive semidefinite, and its null space is exactly two-dimensional, being spanned by $\partial_\tau z(\tau, 0, 0)$ and $\partial_h z(\tau, 0, 0)$.

We can readily deduce the equation for the curve $z_0(\tau)$: since $dz_0(\tau)/d\tau = \partial_\tau z(\tau, 0, 0)$, the curve $\mathcal{O}$ is a solution of ray-tracing equations (3a). By differentiating with respect to τ the basic identities $\partial_\tau z\cdot\nabla\zeta^\mu = 0$, $\partial_h z\cdot\nabla\zeta^\mu = 0$, and $\partial_{\zeta^\nu} z\cdot\nabla\zeta^\mu = \delta_\nu{}^\mu$, one can show that the vector $\partial_\tau\nabla\zeta^\mu(z) + D^2H(z)J_c\nabla\zeta^\mu(z)$, with D^2H denoting the Hessian matrix of H, must be orthogonal to $\partial_\tau z$, $\partial_h z$, and $\partial_{\zeta^\nu} z$ for all ν, hence,

$$\partial_\tau\nabla\zeta^\mu(z) = -D^2H(z)J_c\nabla\zeta^\mu(z).$$

Upon using this identity, we readily obtain an ODE for the matrix $G(\tau)$. Together with the equation for z_0 and for the amplitude $c_0(\tau) = \exp(-2\int_0^\tau \gamma(z_0(\tau'))d\tau')$, this leads to the system of ODEs

$$\frac{dz_0}{d\tau} = -J_c\nabla H(z_0), \quad H(z_0) = 0, \tag{10a}$$

$$\frac{dG}{d\tau} = GJ_cD^2H(z_0) - D^2H(z_0)J_cG, \tag{10b}$$

$$\frac{dc_0}{d\tau} = -2\gamma(z_0)c_0, \tag{10c}$$

In analogy to equations (3), equations (10) are referred to as *phase-space beam-tracing equations* for the case of a quiescent plasma.

We shall now utilize z_0, G, and c_0 to construct a paraxial approximation of the exact Wigner function (9). We consider w^κ as a distribution acting on an arbitrary smooth test-function χ, which vanishes outside a closed and bounded set contained in the domain of definition of the coordinates (τ, h, ζ). Explicitly, we consider the integral

$$\langle w^\kappa, \chi\rangle = \frac{2\pi W_0^\kappa}{\kappa} \int e^{-\kappa|\zeta|_g^2} c(\tau,\zeta)\chi(z(\tau,0,\zeta))J(\tau,0,\zeta)d\tau d\zeta. \tag{11}$$

Here $c(\tau,\zeta) = \exp(-2\int_0^\tau \gamma_H(\tau',\zeta)d\tau')$, and $J(\tau,h,\zeta) > 0$ is the Jacobian determinant of the coordinate transformation $z = z(\tau,h,\zeta)$. The integrand is evaluated at $h = 0$ because of the δ-function in (9). In order to find an asymptotic expansion of this integral in the limit $\kappa \to \infty$, we introduce a simpler coordinate system near the curve $z = z_0(\tau)$ defined by

$$z = \hat{z}(\hat\tau, \hat h, \hat\zeta) = z_0(\hat\tau) + \hat h\theta_h(\hat\tau) + \hat\zeta^\mu\theta_\mu(\hat\tau),$$

where $\hat\tau(z)$ takes values in the same interval $0 \le \tau \le \tau_{\max}$ as before, $\theta_h(\hat\tau) = \partial_h z(\hat\tau,0,0)$, and $\theta_\mu(\hat\tau)$ must be linearly independent of $dz_0(\hat\tau)/d\tau$, $\theta_h(\hat\tau)$, and $\theta_\nu(\hat\tau)$, for $\nu \neq \mu$. Differently from the coordinates (τ,h,ζ), for which the level sets $\tau(z) =$ constant can be curved surfaces, the level sets $\hat\tau(z) =$ constant are planes transversal to the curve z_0 and spanned by the vectors θ_h and $\{\theta_\mu\}_\mu$. In these "planar-cross-section coordinates", the dispersion relation becomes more complicated, that is, $H(\hat z(\hat\tau,\hat h,\hat\zeta)) = 0$; yet, near $z = z_0(\tau)$, it can always be solved for $\hat h$ with the result that $H = 0$ is equivalent to $\hat h = -\hat\zeta^\mu \mathsf{h}_\mu + O(|\hat\zeta|^2)$, with $\mathsf{h}_\mu = \theta_\mu \cdot \nabla H(z_0)$, and thus

$$z(\tau,0,\zeta) = z_0(\hat\tau) + \hat\zeta^\mu\theta_\mu^\perp(\hat\tau) + O(|\hat\zeta|^2),$$

with $\theta_\mu^\perp = \theta_\mu - \mathsf{h}_\mu\theta_h$. (The symbol $\perp$ here refers to the direction perpendicular to $\nabla H(z_0)$, since $\nabla H(z_0)\cdot\theta_\mu^\perp = 0$.) The advantage of the coordinates $(\hat\tau,\hat h,\hat\zeta)$ consists in the freedom of choosing the vectors $\{\theta_\mu\}$ that define the planar cross-sections in phase space.

The integral in (11) can be viewed as an integral over the hypersurface defined implicitly by the dispersion relation $H(z) = 0$, which can be parameterized by either the old coordinates (τ,ζ) or the new coordinates $(\hat\tau,\hat\zeta)$. In order to change variables, we need to compute the Jacobian of the transformation $(\hat\tau,\hat\zeta) \mapsto (\tau,\zeta)$. With this aim we evaluate τ and ζ on the dispersion surface parameterized by $(\hat\tau,\hat\zeta)$ coordinates. First, we have

$$\begin{aligned}\tau &= \tau(z_0(\hat\tau) + \hat\zeta^\mu\theta_\mu^\perp(\hat\tau) + O(|\hat\zeta|^2)) \\ &= \hat\tau + \hat\zeta^\mu\theta_\mu(\hat\tau)\cdot\nabla\tau(z_0(\hat\tau)) + O(|\hat\zeta|^2),\end{aligned}$$

where we used $\tau(z_0(\tau')) = \tau'$ for any τ', and $\theta_\nu^\perp\cdot\nabla\tau(z_0) = \theta_\nu\cdot\nabla\tau(z_0)$, since $\theta_h\cdot\nabla\tau(z_0) = 0$. Analogously,

$$\begin{aligned}\zeta^\mu &= \zeta^\mu(z_0(\hat\tau) + \hat\zeta^\nu\theta_\nu^\perp(\hat\tau) + O(|\hat\zeta|^2)) \\ &= \hat\zeta^\nu\theta_\nu(\hat\tau)\cdot\nabla\zeta^\mu(z_0(\hat\tau)) + O(|\hat\zeta|^2),\end{aligned}$$

since $\zeta^\mu(z_0(\tau')) = 0$ for all τ', and $\theta_\nu^\perp\cdot\nabla\zeta^\mu(z_0) = \theta_\nu\cdot\nabla\zeta^\mu(z_0)$, for all μ. From these identities it follows that

$$\begin{aligned}\partial_{\hat\tau}\tau &= 1 + O(|\hat\zeta|), & \partial_{\hat\zeta^\nu}\tau &= \theta_\nu\cdot\nabla\tau(z_0) + O(|\hat\zeta|), \\ \partial_{\hat\tau}\zeta^\mu &= O(|\hat\zeta|), & \partial_{\hat\zeta^\nu}\zeta^\mu &= \theta_\nu\cdot\nabla\zeta^\mu(z_0(\hat\tau)) + O(|\hat\zeta|).\end{aligned}$$

The leading-order contribution to the Jacobian matrix is upper triangular, so that

$$\det[\partial(\tau,\zeta)/\partial(\hat\tau,\hat\zeta)] = \det\mathsf{T}(\hat\tau) + O(|\hat\zeta|), \tag{12}$$

where $\mathsf{T}_\nu{}^\mu = \theta_\nu\cdot\nabla\zeta^\mu(z_0)$. Using the identities above, we can approximate the factors in the integrand of (11),

$$\begin{aligned}|\zeta|_g^2 &= |\hat\zeta|_{\mathsf{G}}^2 + O(|\hat\zeta|^3), \quad c(\tau,\zeta) = c_0(\hat\tau) + O(|\hat\zeta|), \\ \chi(z(\tau,0,\zeta)) &= \chi(z_0(\hat\tau) + \hat\zeta^\mu\theta_\mu^\perp(\hat\tau)) + O(|\hat\zeta|^2), \\ J(\tau,0,\zeta)d\tau d\zeta &= [\hat J(\hat\tau, -\hat\zeta^\mu\mathsf{h}_\mu, \hat\zeta) + O(|\hat\zeta|)]d\hat\tau d\hat\zeta,\end{aligned}$$

where $|\hat\zeta|_{\mathsf{G}}^2 = \hat\zeta\cdot\mathsf{G}\hat\zeta$, with the matrix $\mathsf{G} = \mathsf{T}g\,{}^t\mathsf{T}$ being related to G by

$$\mathsf{G}_{\mu\nu} = \theta_\mu\cdot G\theta_\nu, \tag{13}$$

and $\hat J$ is the Jacobian of the transformation $z = \hat z(\hat\tau,\hat h,\hat\zeta)$. The derivation of the relation between the Jacobian determinants is not straightforward and deserves a brief digression. On the one hand, we have

$$J(\tau,h,\zeta) = \det(\mathsf{e}_\tau(\tau),\mathsf{e}_h(\tau),\mathsf{e}(\tau)) + O(|\zeta|),$$

where we introduce the covariant basis vectors $\mathsf{e}_\tau(\tau) = \partial_\tau z(\tau,0,0) = dz_0(\tau)/d\tau = \theta_\tau(\tau)$, $\mathsf{e}_h(\tau) = \partial_h z(\tau,0,0) = \theta_h(\tau)$, and $\mathsf{e}(\tau) = (\mathsf{e}_1(\tau),\ldots,\mathsf{e}_{2d-2}(\tau))$, with $\mathsf{e}_\mu(\tau) = \partial_{\zeta^\mu}z(\tau,0,0)$. The vectors $\{\theta_\mu\}$ must be a linear combination of the basis vectors, i.e., $\theta_\mu = U_\mu^\tau\mathsf{e}_\tau + U_\mu^h\mathsf{e}_h + \mathsf{U}_\mu{}^{\mu'}\mathsf{e}_{\mu'}$. We need to determine explicitly only the matrix U, and with this aim, we can scalar-multiply by $\nabla\zeta^\nu(z_0)$, thus obtaining $\mathsf{T}_\mu{}^\nu = \theta_\mu\cdot\nabla\zeta^\nu(z_0) = \mathsf{U}_\mu{}^{\mu'}\delta_{\mu'}{}^\nu$, or $\mathsf{U} = \mathsf{T}$. It follows that the Jacobian determinants of the two coordinate systems, evaluated on the curve $z = z_0(\tau)$, are related by

$$\det(\theta_\tau,\theta_h,\theta) = \det(\mathsf{e}_\tau,\mathsf{e}_h,\mathsf{e})\det\mathsf{T},$$

with $\theta = (\theta_1,\ldots,\theta_{2d-2})$, while we have shown that $d\tau d\zeta = [\det\mathsf{T} + O(|\hat\zeta|)]d\hat\tau d\hat\zeta$, cf. equation (12). Hence the two factors $\det\mathsf{T}$ cancel each other out, and the claimed identity holds on z_0; a first-order Taylor expansion is sufficient to account for the $O(|\hat\zeta|)$ correction, which we introduced so that $\hat J$ is evaluated on the approximated form of the dispersion relation, $\hat h + \hat\zeta^\mu\mathsf{h}_\mu(\hat\tau) = 0$.

All the various remainder in the Taylor expansions can be estimated by the inequality

$$\left|(\hat\zeta_1)^{n_1}\cdots(\hat\zeta_{2d-2})^{n_{2d-2}}e^{-\kappa|\hat\zeta|_{\mathsf{G}}^2}\right| \le C\kappa^{-n/2}, \quad n = \sum_\mu n_\mu, \tag{14}$$

which is the analogous of (2).

We can now change coordinates in equation (11) and use inequality (14), with the result that

$$\begin{aligned}\langle w^\kappa,\chi\rangle = \frac{2\pi W_0^\kappa}{\kappa}\int e^{-\kappa|\hat\zeta|_{\mathsf{G}}^2}c_0(\hat\tau)\chi(z_0(\hat\tau) + \hat\zeta^\mu\theta_\mu^\perp(\hat\tau)) \\ \times\hat J(\hat\tau, -\hat\zeta^\mu\mathsf{h}_\mu(\hat\tau),\hat\zeta)d\hat\tau d\hat\zeta + O\Big(\frac{2\pi W_0^\kappa}{\kappa\sqrt\kappa}\Big),\end{aligned}$$

for any test function χ supported in a neighborhood of the curve $z = z_0(\tau)$. This asymptotic expression can be equivalently written as

$$\langle w^\kappa - w_p^\kappa,\chi\rangle = O\Big(\frac{2\pi W_0^\kappa}{\kappa\sqrt\kappa}\Big), \tag{15a}$$

where

$$w_p^\kappa(z) = \frac{2\pi W_0^\kappa}{\kappa}\delta((z-z_0)\cdot\nabla H(z_0))e^{-\kappa(z-z_0)\cdot G(z-z_0)}c_0, \quad (15b)$$

where z_0, G, and c_0 are evaluated at $\tau = \hat{\tau}(z)$. Therefore, equation (15b) provides an approximation of the exact solution w^κ that can be evaluated given only a solution of system (10). The function $\hat{\tau}$ can also be computed from the knowledge of the curve z_0. We note that the dispersion relation in (15b) has been approximated in such a way that $(z-z_0)\cdot\nabla H(z_0) = \hat{h} + \hat{\zeta}\mathsf{h}_\mu(\hat{\tau}) = 0$, cf. the argument of the δ-function. This approximation could be avoided, but it does not change the order of the remainder term as $\kappa \to +\infty$. The *paraxial Wigner function* (15b) depends on the choice of the vectors θ_μ, as they define implicitly the function $\tau = \hat{\tau}(z)$. One can readily check that (15b) is invariant with respect to transformations of the form $\theta_\mu \mapsto \mathsf{U}_\mu{}^\nu\theta_\nu$, as the function $\hat{\tau}$ is invariant. For a general transformation, w_p^κ changes by a quantity of the same order as the remainder in (15). A similar property holds for the standard pWKB of section 1.1.

2.2 Reconstruction of the beam parameters

Having obtained the paraxial approximation of the Wigner function, we can now extract physics information on the wave beam. The relation between the Wigner function and the wave electric field is given by equation (5) for the correlation matrix ρ^κ of the field evaluated with $W^\kappa = w^\kappa e\,{}^te$, where $e(z)$ is the polarization of the considered wave mode. In the direct numerical approach used in `WKBeam`, the calculation of ρ^κ is generally not needed, since the relevant physical quantities can be computed directly from the Wigner function. With the paraxial solution is however possible to reconstruct an approximation of ρ^κ, and thus have access to more physical information. This reconstruction is also needed to define the initial conditions for equations (10).

Since w^κ is singular, we compute the action of ρ^κ on a suitable matrix-valued test function $\psi(x,x')$, i.e.,

$$\langle\rho^\kappa,\psi\rangle = \int \rho^\kappa(x,x') : \psi(x,x')dxdx' = \langle w^\kappa, \chi_\psi^\kappa\rangle = \langle w_p^\kappa, \chi_\psi^\kappa\rangle + O\Big(\frac{2\pi W_0^\kappa}{\kappa\sqrt{\kappa}}\Big),$$

with $\rho^\kappa : \psi = \sum_{ij}\rho_{ij}^\kappa\psi_{ji}$ and

$$\chi_\psi^\kappa(x,N) = \Big(\frac{\kappa}{2\pi}\Big)^d \int e^{i\kappa N\cdot s}\,{}^te(x,N)\psi(x+\tfrac{s}{2}, x-\tfrac{s}{2})e(x,N)ds,$$

is the transformed test function. We have assumed that ψ is such that χ_ψ^κ is concentrated on z_0 as required to use (15), but otherwise it is an arbitrary test function.

We shall now try to find a suitable change of variables that allows us to transform w_p^κ back from the geometrical-optics phase space to the (x,x') space, thus obtaining a matrix-valued function ρ_p^κ such that $\langle\rho^\kappa,\psi\rangle \approx \langle w_p^\kappa,\chi_\psi^\kappa\rangle \approx \int\rho_p^\kappa : \psi dxdx'$, within the error of the paraxial approximation, for any test function ψ satisfying the assumptions. One difficulty in doing so consists in the fact that, in general, the coordinates (τ,ζ) as well as $(\hat{\tau},\hat{\zeta})$ mix position and refractive-index components. However, under the additional hypothesis (which can fail, e.g., if the curve z_0 undergoes a sharp reflection from a cut-off layer)

$$\nabla_N H(z_0) \neq 0, \quad (16)$$

we can exploit the freedom in the choice of the vectors θ_μ. We choose orthonormal vectors $\mathbb{e}_\alpha(\tau) = \mathbb{e}^\alpha(\tau)$ spanning the plane normal to $\nabla_N H(z_0(\tau))$ in the physical position space, and define $\mathbb{f}_\alpha = -|\nabla_N H(z_0|^{-2}(\mathbb{e}_\alpha\cdot\nabla_x H(z_0))\nabla_N H(z_0)$, and

$$\theta_\mu = \begin{pmatrix}\mathbb{e}_\alpha\\ \mathbb{f}_\alpha\end{pmatrix}, \quad \theta_\nu = \begin{pmatrix}0\\ \mathbb{e}^\alpha\end{pmatrix},$$

where $\mu = \alpha$ and $\nu = d-1+\alpha$, for $\alpha = 1,\dots,d-1$. These vectors satisfy $\theta_\mu\cdot\nabla H(z_0) = 0$, hence $\theta_\mu^\perp = \theta_\mu$. In addition, with $\hat{\zeta} = (y,\eta)$, $y = (y^\alpha)_\alpha$, $\eta = (\eta_\alpha)_\alpha$, we find $\hat{z}(\hat{\tau}, -\hat{\zeta}^\nu\mathsf{h}_\mu(\hat{\tau}),\hat{\zeta}) = \hat{z}(\hat{\tau},0,\hat{\zeta}) = (\hat{x}_h(\hat{\tau},y), \hat{N}_h(\hat{\tau},y,\eta))$ with

$$\begin{cases}\hat{x}_h(\hat{\tau},y) = x_0(\hat{\tau}) + y^\alpha\mathbb{e}_\alpha(\hat{\tau}),\\ \hat{N}^h(\hat{\tau},y,\eta) = N^0(\hat{\tau}) + y^\alpha\mathbb{f}_\alpha(\hat{\tau}) + \eta_\alpha\mathbb{e}^\alpha(\hat{\tau}).\end{cases} \quad (17)$$

We see that, on the dispersion surface (denoted by the sub/superscript h), the spatial coordinates x are now related to $(\hat{\tau},y)$ only, while the refractive index vector at a given position is determined by η (the dispersion relation is implied, so that $d-1$ coordinates are sufficient to determine N). Particularly, $\hat{\tau}$ depends on x only. Then,

$$\begin{aligned}\langle w_p^\kappa,\chi_\psi^\kappa\rangle &= W_0^\kappa\Big(\frac{\kappa}{2\pi}\Big)^{d-1}\\ &\times\int e^{-\kappa(\mathsf{A}_{\alpha\beta}y^\alpha y^\beta + 2\mathsf{B}_\alpha{}^\beta y^\alpha\eta_\beta + \mathsf{C}^{\alpha\beta}\eta_\alpha\eta_\beta) + i\kappa\hat{N}\cdot s}c_0(\hat{\tau})\\ &\times(e(z_0)\,{}^te(z_0)) : \psi(\hat{x}+\tfrac{s}{2},\hat{x}-\tfrac{s}{2})\hat{J}_0(\hat{\tau})dsd\hat{\tau}dyd\eta + \cdots\end{aligned}$$

where $\hat{J}_0(\hat{\tau}) = \hat{J}(\hat{\tau},0,0) = \det(\theta_\tau(\hat{\tau}),\theta_h(\hat{\tau}),\theta(\hat{\tau}))$, the matrix blocks A, B, and C are defined by

$$\mathsf{G} = \begin{pmatrix}\mathsf{A} & \mathsf{B}\\ {}^t\mathsf{B} & \mathsf{C}\end{pmatrix}, \quad (18)$$

and "$\cdots$" stands for the contribution of terms that are at least linear in (y,η). One can show that C is strictly positive definite. The needed change of variable is

$$\begin{cases}x_1(\hat{\tau},y,s) = x_0(\hat{\tau}) + y^\alpha\mathbb{e}_\alpha(\hat{\tau}) + s/2,\\ x_2(\hat{\tau},y,s) = x_0(\hat{\tau}) + y^\alpha\mathbb{e}_\alpha(\hat{\tau}) - s/2,\end{cases}$$

and the corresponding Jacobian matrix is

$$\frac{\partial(x_1,x_2)}{\partial(\hat{\tau},y,s)} = \begin{pmatrix}\frac{dx_0}{d\tau}(\hat{\tau}) + O(|y|) & \mathbb{e}_1 & \dots & \mathbb{e}_{d-1} & \frac{1}{2}I\\ \frac{dx_0}{d\tau}(\hat{\tau}) + O(|y|) & \mathbb{e}_1 & \dots & \mathbb{e}_{d-1} & -\frac{1}{2}I\end{pmatrix}.$$

The determinant can be computed via the Schur complement with the result that

$$\left|\frac{\partial(x_1,x_2)}{\partial(\hat{\tau},y,s)}\right| = J_s(\hat{\tau}) + O(|y|),$$

where $J_s = \det\big(\frac{dx_0}{d\tau},\mathbb{e}_1,\dots,\mathbb{e}_{d-1}\big)$ is the Jacobian determinant of $x = \hat{x}(\tau,y)$, which is the spatial part of the coordinates, evaluated at $y = 0$. Since $\{\frac{dx_0}{d\tau},\mathbb{e}_1,\dots,\mathbb{e}_{d-1}\}$ is an orthogonal basis for the x-space, $|\mathbb{e}_\mu| = 1$ for all μ, and $dx_0/d\tau = \nabla_N H(z_0)$, it follows that the Jacobian satisfies $\big|J_s(\tau)\big| = \big|\nabla_N H(z_0(\tau))\big|$.

With this change of coordinates, we have

$$\langle w_p^\kappa, \chi_\psi^\kappa \rangle = \int \rho_p^\kappa(x_1, x_2) : \psi(x_1, x_2) dx_1 dx_2 + \cdots$$

as desired. Since ψ is an arbitrary test function, ρ_p^κ is an approximation of the distribution ρ^κ. We skip the details of this last step and do not report the general expression of ρ_p^κ as it is not needed. It is sufficient to evaluate ρ_p^κ at points of the form $x_j = x_0(\hat{\tau}) + y_j^\alpha \mathbb{e}_\alpha(\hat{\tau})$ for $j = 1, 2$, that is, on the same cross-section of the beam. The result is

$$\begin{aligned} \rho_p^\kappa(x_1, x_2) = & \frac{(\kappa/4\pi)^{\frac{d-1}{2}} \hat{J}_0 W_0^\kappa c_0}{\big|\nabla_N H(z_0)\big| \sqrt{\det \mathsf{C}}} \big(e(z_0)\, {}^t e(z_0)\big) \\ & \times e^{i\kappa \mathsf{N}_\alpha^0 y_1^\alpha - \frac{\kappa}{4}(\mathsf{A}+\mathsf{D}^s)_{\alpha\beta} y_1^\alpha y_1^\beta} \\ & \times e^{-i\kappa \mathsf{N}_\alpha^0 y_2^\alpha - \frac{\kappa}{4}(\mathsf{A}+\overline{\mathsf{D}^s})_{\alpha\beta} y_2^\alpha y_2^\beta} \\ & \times e^{-\frac{\kappa}{2}(\mathsf{A}-\mathsf{D}^a)_{\alpha\beta} y_1^\alpha y_2^\beta}, \end{aligned} \tag{19}$$

where $\hat{J}_0 = \det(\theta_\tau, \theta_h, \theta)$, whereas $\mathsf{N}_\alpha^0 = N^0 \cdot \mathbb{e}_\alpha$, $\mathsf{D} = \mathsf{C}^{-1}$,

$$\mathsf{D}^s = (\mathsf{I} + i\mathsf{B})\mathsf{D}(\mathsf{I} + i^t\mathsf{B}), \quad \mathsf{D}^a = (\mathsf{I} + i\mathsf{B})\mathsf{D}(\mathsf{I} - i^t\mathsf{B}),$$

with I being the $(d-1)\times(d-1)$ identity matrix, and overbars denote complex conjugation. (We reserve "$*$" for the Hermitian conjugate.) By definition ρ^κ must satisfy the relation $\rho^\kappa(x_2, x_1)^* = \rho^\kappa(x_1, x_2)$ and the approximation (19) indeed does have this property. We can also see that ρ_p^κ comprises the product of a function of $(\hat{\tau}, y_1)$, a function of $(\hat{\tau}, y_2)$, and a function of all variables $(\hat{\tau}, y_1, y_2)$. On the other hand, a correlation matrix ρ^κ corresponds to a pure beam if $\rho^\kappa(x, x') = E^\kappa(x)E^\kappa(x')^*$, where E^κ is a deterministic field (that is, the electric field is given by E^κ with probability one). Therefore, ρ_p^κ corresponds to a pure beam if and only if $\mathsf{A} - \mathsf{D}^a = 0$ or equivalently

$$\mathsf{G}\mathsf{J}_c\mathsf{G} = \mathsf{J}_c, \quad \text{with} \quad \mathsf{J}_c = \begin{pmatrix} 0 & -\mathsf{I} \\ \mathsf{I} & 0 \end{pmatrix}, \tag{20}$$

where J_c is the canonical Poisson tensor in dimension $2(d-1)$. Similarly to the case of wave packets [21], pure wave beams are related to symplectic matrices, but in a more complicated way: for beams the reduced matrix G is symplectic, while the full matrix G is singular. If (20) is satisfied, then (19) reduces to

$$\begin{aligned} \rho_p^\kappa(x_1, x_2) = & \frac{(\kappa/4\pi)^{\frac{d-1}{2}} \hat{J}_0}{\big|\nabla_N H(z_0)\big| \sqrt{\det \mathsf{C}}} W_0^\kappa c_0 \, \big(e(z_0)\, {}^t e(z_0)\big) \\ & \times e^{i\kappa \mathsf{N}_\alpha^0 y_1^\alpha - \frac{\kappa}{2}(\mathsf{C}^{-1} + i\mathsf{B}\mathsf{C}^{-1})_{\alpha\beta} y_1^\alpha y_1^\beta} \, e^{-i\kappa \mathsf{N}_\alpha^0 y_2^\alpha - \frac{\kappa}{2}(\mathsf{C}^{-1} - i\mathsf{B}\mathsf{C}^{-1})_{\alpha\beta} y_2^\alpha y_2^\beta}. \end{aligned} \tag{21}$$

We can compare (21) with the paraxial solution for a Gaussian beam, evaluated at $x = x_0 + y^\alpha \mathbb{e}_\alpha$, cf. section 1.1,

$$E_{\mathrm{GB}}^\kappa(x) = e(z_0) A_0 e^{i\kappa\left(s_0 + \mathsf{N}_\alpha^0 y^\alpha + \frac{1}{2}\mathsf{S}_{\alpha\beta} y^\alpha y^\beta\right) + i\vartheta_0 - \frac{\kappa}{2}\Phi_{\alpha\beta} y^\alpha y^\beta},$$

with $\mathsf{S}_{\alpha\beta} = \mathbb{e}_\alpha \cdot S\mathbb{e}_\beta$, and $\Phi_{\alpha\beta} = \mathbb{e}_\alpha \cdot \Phi \mathbb{e}_\beta$. Therefore, if condition (20) holds, the paraxial approximation ρ_p^κ corresponds to a Gaussian beam with reference ray $x = x_0$, refractive index $N = N^0$, $z_0 = (x_0, N^0)$, and with

$$|A_0|^2 = \frac{(\kappa/4\pi)^{\frac{d-1}{2}} \hat{J}_0 W_0^\kappa c_0}{\big|\nabla_N H(z_0)\big| \sqrt{\det \mathsf{C}}}, \quad \mathsf{S} = -\mathsf{B}\mathsf{C}^{-1}, \quad \Phi = \mathsf{C}^{-1}. \tag{22}$$

The phases s_0 and ϑ_0, however, cannot be recovered in this way, since ρ^κ evaluated at points on the same beam cross-section does not "see" a phase that depends only on τ. Particularly, the beam width is readily obtained from the eigenvalues of C. Then we can see that the amplitude in (21) contains the usual physical effects: the factor $|\nabla_N H(z_0)|^{-1}$ accounts for the change in amplitude due to group velocity, while $\sqrt{\det \mathsf{C}}$ describes the effects of the beam width (focusing/defocusing). The block matrices B and C can be obtained from the solution G via (13) and (18).

Vice-versa we can use the pure state (21) to find the initial conditions for the phase-space beam-tracing equations (10). If the plane $\hat{\tau}(x) = 0$ represents the launching mirror, we impose that at $\hat{\tau} = 0$, ρ_p^κ corresponds to a pure Gaussian beam with given $z_0(0)$, A_0, $\mathsf{S}(0)$ and $\Phi(0)$. Then we have the initial condition for z_0, and deduce the initial values for c_0 and G by inverting (22) and using (20). One can check that the resulting reduced matrix G is symmetric, positive definite as it should be. This does not yet fully determine the initial condition for $2d \times 2d$ matrix G, but only its $(2d-2)\times(2d-2)$ reduced form. However, by construction G has a two-dimensional null space, and we only need to find the directions of the two orthogonal null eigenvectors. One null eigenvector is simply given by $-J_c \nabla H(z_0)$, that is

$$G(\tau) J_c \nabla H(z_0(\tau)) = 0, \quad \text{for all } \tau, \tag{23}$$

since $\partial_\tau z(\tau, 0, 0) = -J_c \nabla H(z_0)$. The other null eigenvector is $\partial_h z(\tau, 0, 0)$ and it cannot be directly computed unless we construct explicitly the coordinate map $z(\tau, h, \zeta)$. However, for the purposes of computing $G(0)$, we only need the second null eigenvector at $\tau = 0$. Under assumption (16), we can choose the initial conditions for the coordinate map $z = z(\tau, h, \zeta)$ so that $\partial_h z(0, 0, 0) = \theta_h(0) = (0, \big|\nabla_N H(z_0(0))\big|^{-2} \nabla_N H(z_0(0)))$ and thus we must have

$$G(0) \begin{pmatrix} 0 \\ \nabla_N H(z_0(0)) \end{pmatrix} = 0. \tag{24}$$

It is possible to show that, given $\mathsf{G}(0)$ from the Gaussian beam parameters, constraints (23) and (24) determine uniquely the initial condition $G(0)$.

We can now summarize the main steps of the phase-space beam-tracing method: Given a launched Gaussian beam, we can use (20) and (22) to find the initial point $z_0(0)$, the initial amplitude $c_0(0)$, and the reduced matrix $\mathsf{G}(0)$. Then, we solve the constraints (23) and (24) for the full matrix $G(0)$. We can then solve system (10), and use (19) to reconstruct the density matrix.

So far scattering has been neglected. Therefore ρ_p^κ should preserve the form of a pure state, since there is no mechanism that can produce a mixed state. It is therefore desirable that condition (20), which holds at $\tau = 0$, remains true for all $\tau \geq 0$. This can be proven rigorously in the two-dimensional case ($d = 2$). A general proof for $d > 2$ is not available, but numerical experiments suggest that solutions of (10b) preserve relation (20).

As an example, we note that in the case of the scalar Helmholtz equation with a linear dielectric function, i.e., $H(x, N) = \frac{1}{2}(N^2 - 1 + b\cdot x)$, equations (10) can be solved analytically. This includes the case of the propagation of an O-mode wave perpendicular to the background magnetic field in a plasma with a linear density profile. Then the blocks of the Hessian matrix $D^2 H$ are (with same notation as in section 1.1) $H_{xx} = H_{xN} = H_{Nx} = 0$ and $H_{NN} = I$, where I is the identity matrix. The solution of (10a) yields parabolic ray trajectories. As for G, if we write

$$G = \begin{pmatrix} A & B \\ {}^t B & C \end{pmatrix},$$

then the solution of (10b) is given by

$$\begin{aligned} A(\tau) &= A(0), \\ B(\tau) &= B(0) - \tau A(0), \\ C(\tau) &= C(0) - \tau[B(0) + {}^t B(0)] + \tau^2 A(0). \end{aligned} \tag{25}$$

This analytical solution indeed preserve condition (20), i.e. $G(\tau)$ satisfies the condition if $G(0)$ does. The standard beam tracing equation (3b) can also be solved analytically [26] and the two solutions yields exactly the same description of the beam (except for the phase which cannot be recovered from the Wigner function).

In the remaining part of this section, we briefly present a selected numerical example. For simplicity, we consider a beam of electromagnetic waves with frequency $f = \omega/2\pi = 100$ GHz (so that $k_0 = \omega/c = 20\ \mathrm{cm}^{-1}$) in an isotropic plasma. The Hamiltonian is $H(x, N) = \frac{1}{2}[N^2 - 1 + \omega_{p,e}^2(x)/\omega^2]$, where $\omega_{p,e}^2(x) = 4\pi q_e^2 n_e(x)/m_e$ is the electron plasma frequency at the point x, whereas q_e and m_e are the electric charge and the mass of an electron, respectively. Although the dispersion relation has been simplified by neglecting the confining magnetic field, we consider a realistic three-dimensional geometry ($d = 3$), with electron density

$$n_e(x) = n_{e,1}(1 - (r/a)^2), \quad \text{for } 0 \le r < a, \tag{26}$$

and $n_e(x) = 0$ for $r \ge a$, with

$$x = \begin{pmatrix} x^1 \\ x^2 \\ x^3 \end{pmatrix} = \begin{pmatrix} [R_0 + r\cos(\vartheta)]\cos(\varphi) \\ [R_0 + r\cos(\vartheta)]\sin(\varphi) \\ r\sin(\vartheta) \end{pmatrix}. \tag{27}$$

For the density model, we choose $R_0 = 150$ cm, $a = 50$ cm, and $n_{e,1} = 10^{14}\ \mathrm{cm}^{-3}$. The launch point of the beam is $x_0(0) = (R_0 + a, 0, 0)$, with initial refractive index $N^0(0) = (-\cos\vartheta_b\cos\phi_b, \cos\vartheta_b\sin\varphi_b, \sin\vartheta_b)$, which gives the direction of the beam, with poloidal and toroidal launch angles $\vartheta_b = 10°$ and $\varphi_b = 15°$, respectively. The beam widths are $W_1 = 2$ cm and $W_2 = 2.5$ cm in the directions $(-\sin\vartheta_b\cos\varphi_b, \sin\vartheta_b\sin\varphi_b, -\cos\vartheta_b)$ and $(-\sin\varphi_b, -\cos\varphi_b, 0)$, respectively. The phase-front radii of curvature are $R_1 = -100$ cm and $R_2 = -40$ cm in the same two directions as the beam widths, respectively (negative values signify focusing). Figure 1 shows a comparison between the standard beam-tracing solution, equations (3), and the phase-space beam-tracing solution, equations (10). In the upper panels the projections of the beam onto the poloidal and toroidal planes are shown together with a color map representing the electron density (26). The projections are obtained by integrating the beam energy density in the direction which is projected out. Lower panels show the beam parameters computed from (22). We can see that in absence of density fluctuations the phase-space and the standard beam tracing results are in agreement. Quantitatively, condition (20) and the constraint (23) are satisfied within an error of 10^{-8} and 10^{-11}, respectively; the difference between the beam parameters in the two descriptions cannot be appreciated from the figure as it is smaller than 10^{-8}. This shows that the phase-space and the standard beam-tracing description of the beam are essentially equivalent in absence of density fluctuations. The advantage of the phase-space approach consists in the possibility of accounting for density fluctuations, as discussed in the next section.

3 Phase-space beam tracing with diffusive scattering

The strategy followed in section 2 for the case without fluctuations relies on the exact analytical solution (9) in an adapted coordinate system. For the complete wave kinetic equation (6), including the scattering term due to the fluctuations, we do not have a general analytic solution, and thus, instead of approximating the solution directly, we look for approximate solutions of the equation, using (9) as a guide to formulate a suitable ansatz. This is a standard method in asymptotic analysis, but we note that it is weaker than the direct approach of section 2: the fact that the equation is almost satisfied by the approximate solution does not imply that the approximate solution converges to the exact one. The considered ansatz for the paraxial solution reads

$$w_p^\kappa(\tau, h, \zeta) = \frac{2\pi}{\kappa}\delta(h)c(\tau,\zeta)e^{-\kappa|\zeta|_g^2} = \frac{2\pi}{\kappa}\delta(h)v_p^\kappa(\tau,\zeta), \tag{28}$$

where (τ, h, ζ) are curvilinear coordinates with $h = H$ and with (τ, ζ) to be determined; as before, $|\zeta|_g^2 = \zeta \cdot g\zeta$ with the symmetric, positive definite matrix g to be determined. Ansatz (28) is substituted into (6), and imposing that the leading-order terms vanish leads to equations for the central curve $z = z_0(\tau)$ defined by the conditions $h = 0$ and $\zeta = 0$, and for the evolution of $c_0(\tau) = c(\tau, 0)$ and $\nabla\zeta^\mu(z_0)$ along it. The key point in this derivation is the treatment of the scattering operator (7). We can write

$$S^\kappa(w_p^\kappa) = \frac{2\pi}{\kappa}\delta(h)\Big[\mathbb{D}_{\alpha\beta}^\kappa\frac{\partial^2 v_p^\kappa}{\partial\eta_\alpha\partial\eta_\beta} + S_r^\kappa + O(\sqrt{\kappa})\Big], \tag{29}$$

where the coordinates (y, η) are defined as in section 2, and

$$\mathbb{D}_{\alpha\beta}^\kappa = \frac{1}{\kappa}\frac{\sqrt{\pi/2}}{|\nabla_N H(z_0)|}\frac{|e^*(z_0)\varepsilon_F(x_0)e(z_0)|^2 F(x_0)^2}{\sqrt{\det\Xi(x_0)\det K(x_0)}}(K(x_0)^{-1})_{\alpha\beta},$$
$$K^{\alpha\beta} = \mathbb{e}^\alpha(\tau)\cdot\Xi(x_0(\tau))^{-1}\mathbb{e}^\beta(\tau),$$

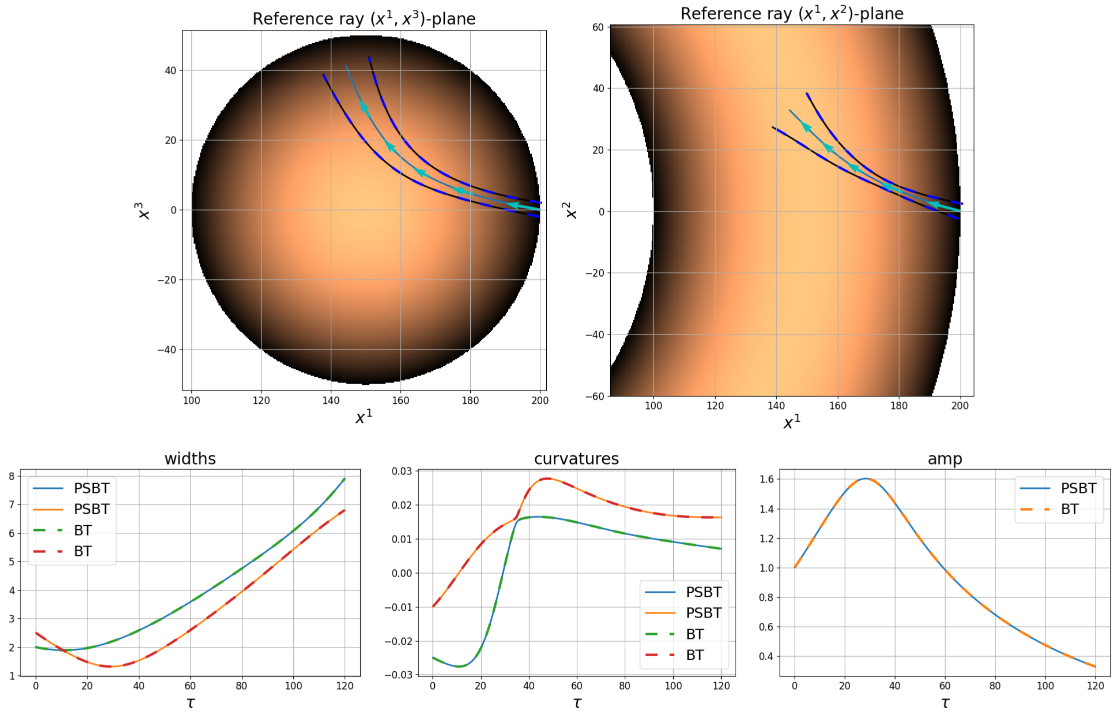

Figure 1. Phase-space beam-tracing (PSBT) solution versus the standard beam-tracing (BT) solution for the case of a Gaussian beam in the model equilibrium defined by equation (26), without density fluctuations. Top panels show (from left to right) the projections of the reference ray $x = x_0$ and the "beam boundaries" into the x^1-x^3 (poloidal) and x^1-x^2 (toroidal) plane. The bottom panels show (from left to right) the beam widths, the phase-front curvatures, and the amplitudes. The continuous and dashed lines correspond to the phase-space and the standard beam-tracing results, respectively.

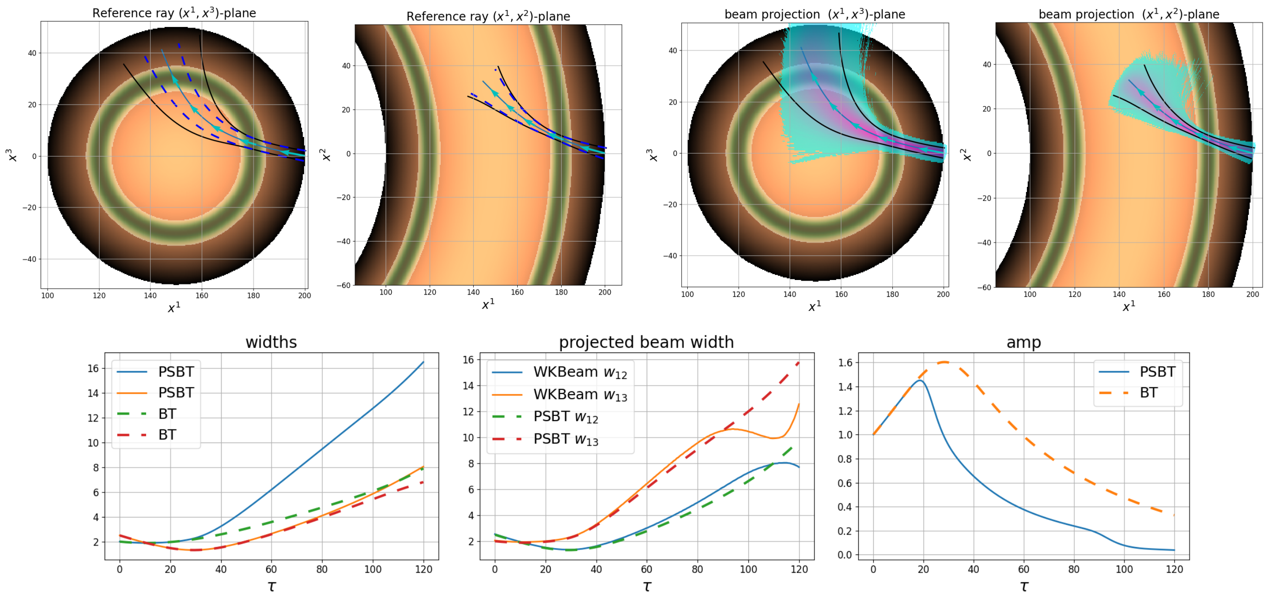

Figure 2. Phase-space beam tracing (PSBT) solution versus the standard beam-tracing (BT) solution and the direct numerical solution of the wave kinetic equation (6) obtained by the `WKBeam` code for the same case as in figure 1, but with density fluctuations in the diffusive scattering regime. The green color map show the profile of the root mean square of relative density fluctuations according to equation (32). Top panels show the poloidal and toroidal projections of the beam compared to the standard beam tracing (left-hand side panels) and to the `WKBeam` intensity (right-hand side panels). Beam widths and amplitude profiles, computed from equation (31), are shown in the bottom panels.

with F and Ξ being defined in equation (4), $e(z)$ is the polarization unit vector, $\mathbb{e}^\alpha$ is defined in equation (17), and $\varepsilon_F = \varepsilon_{\text{cold}} - I$, cf. equation (7) and the definition of σ^κ. The first term in (29) describes a diffusion process in refractive-index space. The whole operator however also has an integral part S_r^κ that accounts for large deviations of the refractive index vector (the precise expression is not needed here). We restrict our analysis to the diffusive scattering regime [19], in which we can neglect the integral part S_r^κ.

Then we find that in presence of fluctuations in the diffusive scattering regime, the phase-space beam-tracing equations (10) become

$$\frac{dz_0}{d\tau} = -J_c \nabla H(z_0), \quad H(z_0) = 0, \tag{30a}$$
$$\frac{dG}{d\tau} = GJ_c D^2 H(z_0) - D^2 H(z_0) J_c G - 2G\Delta G, \tag{30b}$$
$$\frac{dc_0}{d\tau} = -(2\gamma(z_0) + \mathrm{tr}(\Delta G))c_0, \tag{30c}$$

where $\mathrm{tr}(\cdot)$ denotes the trace of a matrix, and

$$\Delta = \sqrt{2\pi} \frac{|e^*(z_0)\varepsilon_F(x_0)e(z_0)|^2 F(x_0)^2}{|\nabla_N H(z_0)| \sqrt{\det \Xi(x_0) \det K(x_0)}} \begin{pmatrix} 0 & 0 \\ 0 & \Delta_{NN} \end{pmatrix},$$

with $\Delta_{NN} = (K(x_0)^{-1})_{\alpha\beta} \mathbb{e}^\alpha \otimes \mathbb{e}^\beta$. With respect to (10), the only difference is the additional term in (30b), which changes the evolution of the matrix G. This determine a variation of the width of the Wigner distribution in phase-space, and a corresponding change in the amplitude c_0, which now depends on G, cf. equation (30c). The addition of the scattering terms breaks condition (20), i.e. the matrix G is no longer symplectic and the Wigner function, in general, does not describe a pure beam. One can still use equation (19). For instance the statistically averaged electric-field energy density is proportional to

$$\mathrm{tr}\, \rho_p^\kappa(x, x) = \frac{(\kappa/4\pi)^{\frac{d-1}{2}} \hat{J}_0 W_0^\kappa c_0}{\left|\nabla_N H(z_0)\right| \sqrt{\det \mathsf{C}}} e^{-\kappa(\mathsf{A}-\mathsf{BD}^t\mathsf{B})_{\alpha\beta} y^\alpha y^\beta}, \tag{31}$$

where $x = x_0(\tau) + y^\alpha \mathbb{e}_\alpha(\tau)$, so that the width of the the "beam" can still be computed from the matrix $\mathsf{A} - \mathsf{BD}^t\mathsf{B}$ similarly to the case of pure beams. One should however keep in mind that, in presence of fluctuations, the Wigner function does not describe a specific wave beam, but rather the correlation function of many random perturbations of a beam. Therefore quantities related to the curvature of the phase fronts are no longer well-defined.

As an example, figure 2 shows the solution of equations (30) for the same case as in figure 1, but with density fluctuations characterized by the Gaussian correlation function (4). In this test, we have chosen the root mean square of density fluctuations

$$F(x) = F_0 e^{-(r-r_0)^2/\delta_r^2}, \tag{32}$$

with $r_0 = 30$ cm and $\delta_r = 5$ cm. The constant F_0 is chosen so that the maximum physical root mean square of relative density fluctuations is 10% of the local equilibrium density, i.e., $F_0/\sqrt{\kappa} = 0.1$. The matrix Ξ is determined by constant correlation lengths $L_\parallel = 10^6$ cm, $L_\perp = 5$ cm, with the parallel direction being given by the toroidal angle, i.e. $e_\parallel = e_\varphi = (\cos\varphi, \sin\varphi, 0)$. This highly anisotropic model is meant to emulate the flute-mode character of fluctuations in tokamak plasmas, with the toroidal direction e_φ playing the role of the direction of the confining magnetic field (absent in the model). The perpendicular correlation length $L_\perp$ is larger than the initial beam widths, and this should ensure that the diffusive scattering approximation holds [19].

The effect of the scattering terms in equation (30b) can be clearly appreciated in the poloidal and toroidal projections, figure 2, top-left panels. We see that the beam broadens significantly as compared to the standard beam-tracing solution, which does not account for scattering effects. The broadening is mostly in the poloidal direction. This is due to the strong anisotropy of the correlation function (4). The broadening in toroidal direction is however visible, even though the correlation length in toroidal direction is very large. This is due to the astigmatism of the beam. Figure 2 top-right panels show the comparison of the phase-space beam-tracing solution with the result of the `WKBeam` code, which we regard as the high-fidelity solution. Qualitatively we observe a reasonably good agreement. The `WKBeam` projected energy density shows some non-paraxial effects on the tails of the beam, but the central part of the beam appears well described by the paraxial approximation. More quantitatively, figure 2 bottom-left panel shows the beam widths computed from (31) compared to the beam widths obtained by the standard beam tracing method. The broadening due to the effects of fluctuations is clear. The phase-space and the standard beam-tracing widths begin to deviate at the value of τ for which the beam enters the fluctuation layer, and the deviation is cumulative: the beam width continues to grow after the transit through the fluctuation layer. One can compute the cross-sections of the projected beam for both the paraxial and the `WKBeam` solutions, and then compute the width of the intensity by fitting a Gaussian profile to each τ = constant cross-section of the projected field. In this way we obtain the four profiles shown in figure 2 bottom-center panel. The label W_{ij} refers to the beam width of the projection into the plane x^i-x^j. We see that the phase-space beam-tracing widths follow the `WKBeam` results, but with a visible error, which can be attributed to the non-paraxial effects. (The large deviations visible for $\tau > 80$ are due to loss of resolution near the end-point of the beam in the `WKBeam` solution.) The broadening of the beam implies a reduction of the amplitude due to conservation of the energy flux. This is shown in figure 2 bottom-right panel.

4 Conclusions

In this paper, we have shown how the ideas of Pereverzev's paraxial WKB method can be applied to construct an approximation of the solution of the wave kinetic equation for beams in fluctuating plasmas. The proposed method can be viewed as a beam-tracing method in the geometrical-optics phase space. In section 2, we have described the derivation of the paraxial solution of the wave kinetic equation in a quiescent medium, i.e. without fluctuations. In this case, numerical evidence suggests that this construction is equivalent to the standard pWKB method, as it should be. In the quiescent case, the Wigner function should preserve the purity of the beam. We find that this property is linked to a geometric condition, equation (20), which is the analog for wave beams of the condition previously found for wave packets [21]. The interesting case, however, is that of fluctuating media. In section 3, we reported, without the details of the derivation, the phase-space beam-tracing equations for random media in the diffusive scattering regime, equations (30), and we have discussed a numerical example. We can conclude that, while some details of the electric-field energy density are lost, the paraxial approximation, in all considered tests, appears to provide a reasonably precise estimate of physically relevant quantities, at the cost of the solution of a small system of ODEs. With respect to the Monte Carlo scheme implemented in the `WKBeam` code, the computational speed-up is very substantial: the typical run time of the `WKBeam` code is of the order of one hour on $\approx$ 100 cores; the run time of the current implementation of the paraxial approach (in python, using numpy [27] and scipy [28]) is of the order of one second on a single core. One important drawback is the assumption of diffusive scattering. This is not controlled by the semiclassical parameter κ; it is a rather an *ad hoc* simplification of the scattering operator. When the conditions of validity of this *ad hoc* approximation are not well satisfied, the accuracy of the method is reduced significantly. The extension of the paraxial approach beyond the diffusive regime appears possible [18, 19], since we can compute analytically the action of the full scattering operator on the paraxial Gaussian ansatz (28), the result being another Gaussian with different parameters. This analytical calculation can be used in combination with a splitting method to obtain a heuristic scheme, but this requires further investigation.

Differently from the case of the standard beam tracing method for which appropriate boundary conditions describing reflection at the wall are available [29], both the `WKBeam` code and the new paraxial approximation are so far limited to single-pass absorption, i.e., damping is assumed to be sufficiently strong to absorb completely the wave before it reaches the wall, so that no reflecting boundary conditions have been implemented. However, there is no theoretical obstruction to the inclusion of wall reflections in the future.

References

[1] G.V. Pereverzev, Use of the multidimensional WKB method to describe propagation of lower hybrid waves in tokamak plasma, Nuclear Fusion **32**, 1091 (1992). https://doi.org/10.1088/0029-5515/32/7/I01

[2] G.V. Pereverzev, Paraxial WKB Solution of a Scalar Wave Equation, (Consultants Bureau, New York, 1996)

[3] G.V. Pereverzev, Beam tracing in inhomogeneous anisotropic plasmas, Physics of Plasmas **5**, 3529 (1998). https://dx.doi.org/10.1063/1.873070

[4] E. Poli, A. Peeters, G. Pereverzev, TORBEAM, a beam tracing code for electron-cyclotron waves in tokamak plasmas, Computer Physics Communications **136**, 90 (2001). https://dx.doi.org/10.1016/S0010-4655(01)00146-1

[5] E. Poli, A. Bock, M. Lochbrunner, O. Maj, M. Reich, A. Snicker, A. Stegmeir, F. Volpe, N. Bertelli, R. Bilato et al., TORBEAM 2.0, a paraxial beam tracing code for electron-cyclotron beams in fusion plasmas for extended physics applications, Computer Physics Communications **225**, 36 (2018). https://doi.org/10.1016/j.cpc.2017.12.018

[6] N. Bertelli, O. Maj, E. Poli, G.V. Pereverzev, Y. Peysson, J. Decker, Analysis of the spectral width and validation of the LHBEAM code, AIP Conference Proceedings **1069**, 259 (2008). https://dx.doi.org/10.1063/1.3033710

[7] V.H. Hall-Chen, F.I. Parra, J.C. Hillesheim, Beam model of Doppler backscattering, Plasma Physics and Controlled Fusion **64**, 095002 (2022). https://dx.doi.org/10.1088/1361-6587/ac57a1

[8] C. Tsironis, A.G. Peeters, H. Isliker, D. Strintzi, I. Chatziantonaki, L. Vlahos, Electron-cyclotron wave scattering by edge density fluctuations in ITER, Physics of Plasmas **16**, 112510 (2009). https://dx.doi.org/10.1063/1.3264105

[9] C. Tsironis, P. Papagiannis, F. Bairaktaris, S.I. Valvis, K. Hizanidis, Modelling effects of edge density fluctuations on electron-cyclotron current drive used for neoclassical tearing mode stabilization, Journal of Plasma Physics **87**, 905870103 (2021). https://doi.org/10.1017/S002237782000149X

[10] E.V. Sysoeva, F. da Silva, E.Z. Gusakov, S. Heuraux, A.Y. Popov, Electron cyclotron resonance heating beam broadening in the edge turbulent plasma of fusion machines, Nuclear Fusion **55**, 033016 (2015). https://doi.org/10.1088/0029-5515/55/3/033016

[11] O. Chellaï, S. Alberti, M. Baquero-Ruiz, I. Furno, T. Goodman, F. Manke, G. Plyushchev, L. Guidi, A. Koehn, O. Maj et al., Millimeter-wave beam scattering by field-aligned blobs in simple magnetized toroidal plasmas, Phys. Rev. Lett. **120**, 105001 (2018). https://doi.org/10.1103/PhysRevLett.120.105001

[12] M.W. Brookman, M.E. Austin, C.C. Petty, R.J. La Haye, K. Barada, T.L. Rhodes, Z. Yan, A. Köhn, M.B. Thomas, J. Leddy et al., Resolving ECRH deposition broadening due to edge turbulence in DIII-D, Physics of Plasmas **28**, 042507 (2021). 10.1063/1.5140992

[13] S.W. McDonald, Wave kinetic equation in a fluctuating medium, Phys. Rev. A **43**, 4484 (1991). https://doi.org/10.1103/PhysRevA.43.4484

[14] H. Weber, Ausbreitung hochfrequenter Wellen in fluktuierenden Plasmen (2013), (in English). https://hdl.handle.net/11858/00-001M-0000-0026-E19B-F

[15] H. Weber, O. Maj, E. Poli, Scattering of diffracting beams of electron cyclotron waves by random density fluctuations in inhomogeneous plasmas, EPJ Web of Conferences **87**, 01002 (2015). https://dx.doi.org/10.1051/epjconf/20158701002
[16] A. Snicker, E. Poli, O. Maj, L. Guidi, A. Köhn, H. Weber, G.D. Conway, M. Henderson, G. Saibene, Interaction of the electron density fluctuations with electron cyclotron waves from the equatorial launcher in ITER, Plasma Physics and Controlled Fusion **60**, 014020 (2018). https://doi.org/10.1088/1361-6587/aa8f1a
[17] A. Snicker, E. Poli, O. Maj, L. Guidi, A. Köhn, H. Weber, G. Conway, M. Henderson, G. Saibene, The effect of density fluctuations on electron cyclotron beam broadening and implications for ITER, Nuclear Fusion **58**, 016002 (2018). https://doi.org/10.1088/1741-4326/aa8d07
[18] H. Weber, O. Maj, E. Poli, Wigner-function-based solution schemes for electromagnetic wave beams in fluctuating media, Journal of Computational Electronics **20**, 2199 (2021). https://doi.org/10.1007/s10825-021-01791-8
[19] H. Weber, O. Maj, E. Poli, Paraxial beams in fluctuating fusion plasmas: Diffusive limit and beyond, EPJ Web Conf. **277**, 01003 (2023). https://doi.org/10.1051/epjconf/202327701003
[20] E.V. Sysoeva, E.Z. Gusakov, S. Heuraux, Transition into diffusive regime of propagation of probing electromagnetic waves in a turburlent inhomogeneous plasma and limitations for microwave reflectometry in reactor scale devices, Plasma Physics and Controlled Fusion **55**, 115001 (2013). https://doi.org/10.1088/0741-3335/55/11/115001
[21] E.M. Graefe, R. Schubert, Wave-packet evolution in non-Hermitian quantum systems, Phys. Rev. A **83**, 060101 (2011). https://doi.org/10.1103/PhysRevA.83.060101
[22] G.V. Permitin, A.I. Smirnov, Quasioptics of smoothly inhomogeneous isotropic media, Zh. Eksp. Teor. Fiz. (JETP) **109**, 736 (1996).
[23] V.P. Maslov, The Complex WKB Method for Nonlinear Equations I: Linear Theory, (Birkhäuser, Basel, 1994)
[24] E. Poli, G. Pereverzev, A. Peeters, M. Bornatici, EC beam tracing in fusion plasmas, Fusion Engineering and Design **53**, 9 (2001). https://dx.doi.org/10.1016/S0920-3796(00)00471-3
[25] L. Ryzhik, G. Papanicolaou, J.B. Keller, Transport equations for elastic and other waves in random media, Wave Motion **24**, 327 (1996). https://dx.doi.org/10.1016/S0165-2125(96)00021-2
[26] O. Maj, G.V. Pereverzev, E. Poli, Validation of the paraxial beam-tracing method in critical cases, Physics of Plasmas **16**, 062105 (2009). https://dx.doi.org/10.1063/1.3155449
[27] C.R. Harris, K.J. Millman, S.J. van der Walt, R. Gommers, P. Virtanen, D. Cournapeau, E. Wieser, J. Taylor, S. Berg, N.J. Smith et al., Array programming with NumPy, Nature **585**, 357 (2020). https://doi.org/10.1038/s41586-020-2649-2
[28] P. Virtanen, R. Gommers, T.E. Oliphant, M. Haberland, T. Reddy, D. Cournapeau, E. Burovski, P. Peterson, W. Weckesser, J. Bright et al., SciPy 1.0: Fundamental Algorithms for Scientific Computing in Python, Nature Methods **17**, 261 (2020). https://doi.org/10.1038/s41592-019-0686-2
[29] E. Poli, A.G. Peeters, G.V. Pereverzev, Boundary conditions for a gaussian wave beam, Physics of Plasmas **8**, 4325 (2001). https://dx.doi.org/10.1063/1.1401116